Asian Journal of Chemistry; Vol. 35, No. 4 (2023), 942-950

ASIAN JOURNAL OF CHEMISTRY

https://doi.org/10.14233/ajchem.2023.27585

A Recoverable PANI/α-Fe_2O_3 Nanocatalyst for Ultrasound-Assisted Knovenagel Condensation

MANISHA A. BORA[1,2,*], VASANT V. CHABUKSWAR[1] and MANU VASHISHTHA[3]

[1]Ness Wadia Nanomaterial Research Centre, Department of Chemistry, Nowrosjee Wadia College (Affiliated to S.P. Pune University), Pune-411001, India
[2]Department of Chemistry, BJS's A.S.C. College (Affiliated to S.P. Pune University), Wagholi, Pune-412207, India
[3]Department of Chemical Engineering, Indian Institute of Technology Bombay, Powai, Mumbai-400076, India

*Corresponding author: E-mail: bmanishabora@gmail.com

Received: 18 January 2023; *Accepted*: 27 February 2023; *Published online*: 30 March 2023; AJC-21194

In this research work, a new PANI/α-Fe_2O_3 (PANI = polyaniline) nanocatalyst was prepared and applied to ultrasound-assisted Knoevenagel condensation reaction using ultrasound waves at ambient temperature. The ultrasound-assisted synthesis is a quick, green and efficient C–C bond formation reaction method. Many parameters of the condensation reaction were optimized, such as irradiation time, types of solvent, screening of catalyst and its amount. The results showed that the yields from the ultrasound-assisted reactions were higher than from non-irradiated responses as well as other conventional routes of synthesis. The prepared catalyst was characterized *via* SEM-EDS, FTIR, DLS and XRD studies. The stability and catalytic performance of the PANI/α-Fe_2O_3 were good and it could be reused six times without loss in catalytic activity. The dinitrile molecules were synthesized by Knoevenagel condensation and characterized by FTIR and NMR techniques. Compared to the reported work, the present protocol has numerous benefits such as economical, simplistic workup, high yields and, an environmentally gentle method with a shorter reaction time.

Keywords: Hematite, PANI, Catalysis, Reusability, Nanocomposite, Condensation.

INTRODUCTION

Ultrasound irradiation has been widely accepted as a modern tool in synthetic organic chemistry. The ultrasound synthesis has several advantages such as enhanced reaction rates, pure products with high yields, minimum wastage and short reaction time when compared with the conventional methods [1-4]. The use of ultrasound in conjunction with a heterogeneous catalyst is one of the innovative strategies that has lately drawn a lot of attention [5]. Thus, the development of ultrasonic wave mediated synthesis route for the chemical transformations under milder reaction conditions is highly desirable to avoid harsh reaction conditions followed in conventional routes of synthesis [6-8]. The use of sound energy to promote organic transformations has developed enormously over the last two decades. A variety of ultrasonic mediated cross-coupling reactions featuring good atom economy have emerged as efficient methods for the construction of C–C bonds [9].

Polymeric semiconducting organic materials like polyaniline (PANI) and their transition metal nanocomposites find extensive applications in sensors, catalysis, solar batteries, anti-corrosion coating, supercapacitors [10-12]. Transition metal oxides and their polyaniline based nanocatalytic systems have the potentiality to provide an eco-friendly route for various commercially and biologically important organic molecules [13]. Due to the enormous commercial significance of organic catalysts in recent years, many researchers have concentrated on enhancing their efficiency [14]. The Knoevenagel condensation is one of the best reactions in organic chemistry for the syntheses of small molecules and valuable intermediates of many interesting molecules. The carbon-carbon (C-C) bond formation is the essence of synthetic chemistry and provides the basis for the preparation of more complicated building blocks of organic molecules from simpler ones [15]. The C-C bond formation using transition metal catalysis finds applications in a wide variety of areas such as agrochemicals, pharmaceuticals and organic synthesis [16-19]. The Knoevenagel condensation of carbonyl compounds with active methylene compounds is a classic general method for the preparation of valuable intermediates. Recently, various methodologies have been developed

for Knovenagel condensation [20-22], particularly because of the disadvantages associated with some of the reported procedures. The reported protocols face limitations such as the requirement of hazardous solvents, expensive reagents, higher temperature, longer reaction time, costly, moisture-sensitive catalysts and poor yields. It is desirable to develop efficient, economical and environmentally benign synthetic protocols in neutral media.

The α-Fe_2O_3 (HAM_3) nanoparticles coated with polymer as catalysts have gained much interest in organic transformations [23]. The nature of supporting materials on which nanoparticles are stabilized plays an important role in catalysis as it provides a highly active catalyst surface, which increases the rate of reaction and helps to decrease the use of an amount of catalyst in reaction [24-26]. Unsaturated dinitriles display various biological properties such as antitumor, antimalarial, antifungal, analgesic, antiallergic and antiproliferative [27]. They act as synthetically important intermediates in the synthesis of various biologically important heterocyclic molecules like benzopyran, pyran derivatives, pyridine, cyanohydrins, chromene and also for many other commercially important organic molecules. Herein, an competent ultrasonic cost-effective path in a neutral medium for the synthesis of α,β-unsaturated dicyano compounds *via* Knoevenagel condensation by using PANI/α-Fe_2O_3 nanocomposite as catalyst in aqueous ethanol at room temperature is reported. It was observed that ultrasonic condensation of malanonitrile with various aromatic aldehydes in presence of recyclable PANI/HAM_3, gives highly pure aryl malononitriles with good yields in a short period. The heterogenous PANI/HAM_3 catalyst was prepared by the facile and eco-friendly ultrasonic method. The catalyst can be recycled at least up to six cycles without loss in its efficiency for minimum five times. The products *i.e.* α,β-unsaturated nitriles synthesized by the ultrasonic method have remarkable viable applications in the synthesis of biologically active heterocyclic compounds as precursor.

EXPERIMENTAL

All the chemicals required in the experimental work were of analytical grade (AR) grade and used without further purification except aniline, which was double distilled before its use in the polyaniline composite synthesis. Ferric chloride hexahydrate ($FeCl_3 \cdot 6H_2O$), cetyl trimethyl ammonium bromide (CTAB), aniline (99% monomer), ammonium persulphate (APS), HCl, aromatic aldehydes, malononitrile were purchased from Sigma-Aldrich, USA. Deionized water was used for the preparation of all solutions required for catalyst synthesis.

Characterization: Fourier transform infrared spectroscopy (FTIR) analysis was performed with Perkin-Elmer 160 FTIR Spectrophotometer in the range of 4000-400 cm^{-1}. Powder X-ray diffraction (XRD) studies were done on Philips PW 172Q X-ray diffractometer with Cu*K*α radiation (λ = 1.54 Å). The nanodimensions and morphology were investigated by field emission scanning electron microscope (FESEM) by FEI-Nova Nano SEM 450 and transmission electron microscopy (TEM) in JEOL, JEM2200FS. The ^{1}H NMR (500 MHz) spectra obtained on Bruker AV 500 spectrophotometer in DMSO-d_6, chemical shifts are reported in ppm from tetramethyl silane (TMS).

Hydrothermal synthesis of α-Fe_2O_3 (HAM_3) nanoparticles using CTAB as template: Aqueous solution (10 mL) of cetyltrimethylammonium bromide surfactant (0.01%) was stirred by adding to 0.1 M (50 mL) aqueous solution of $FeCl_3 \cdot 6H_2O$. Then aqueous NH_3 (25%) was added dropwise to it till the pH of solution becomes alkaline (pH ~10) by keeping the solution in an ultrasonic bath for 30 min. The brown-red slurry obtained was sonicated further for 30 min and then heated hydrothermally at 200 ºC for 6 h. The brick-red precipitate obtained was cooled and sonicated for 15 min, filtered, washed several times with deionized water followed by ethanol and dried. The sample was then kept in an oven at about 60 ºC for 24 h to get dry red iron oxide *i.e.* HAM_3 nanoparticles (**Scheme-I**).

Ultrasonic synthesis of PANI/HAM_3 nanocomposites: An aqueous (1 M) solutions of aniline and HCl (1:1 molar ratio) were mixed by cooling in an ice bath (0-5 ºC) and stirred ultrasonically for 30 min. To this solution, HAM_3 nanoparticles (20%w/w) were dispersed uniformly *via* ultrasonication to avoid agglomeration of nanoparticles. An aqueous solution of APS (1.6 mmol) was added gradually to the above mixture with constant stirring and cooling at 0-5 ºC. Then, the solution was continuously sonicated for 6 h at room temperature to get the polyaniline/α-Fe_2O_3 nanocomposite. The resulting dark green precipitate was filtered, washed with deionized water and dried in vacuum at 60-70 ºC for 24 h to get dark green dry powder of PANI/HAM_3 nanocomposite (**Scheme-II**).

Ultrasonic synthesis of control reaction: A Pyrex-glass closed vessel was charged with *p*-chloro benzaldehyde (1 mmol), malononitrile (1 mmol) and PANI/HAM_3 (20 mg) in 50% (v/v) aqueous ethanol (5 mL) and irradiated in an ultrasonic bath (45 kHz). The reaction mixture was sonicated at room temperature for the appropriate time. The progress of the reaction was monitored by TLC (petroleum ether:ethyl acetate 20:80). After the completion of the reaction, PANI/HAM_3 nanocatalyst was separated by centrifugation followed by filtration. The filtrate obtained was poured in cold water to get a solid precipitate of product. The crude solid product obtained was further purified by simple recrystallization and then dried in oven at about 60-70 ºC for 24 h (**Scheme-III**).

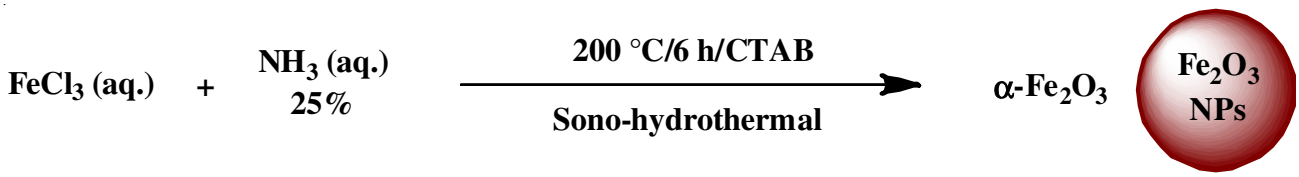

Scheme-I: Hydrothermal synthesis of HAM_3

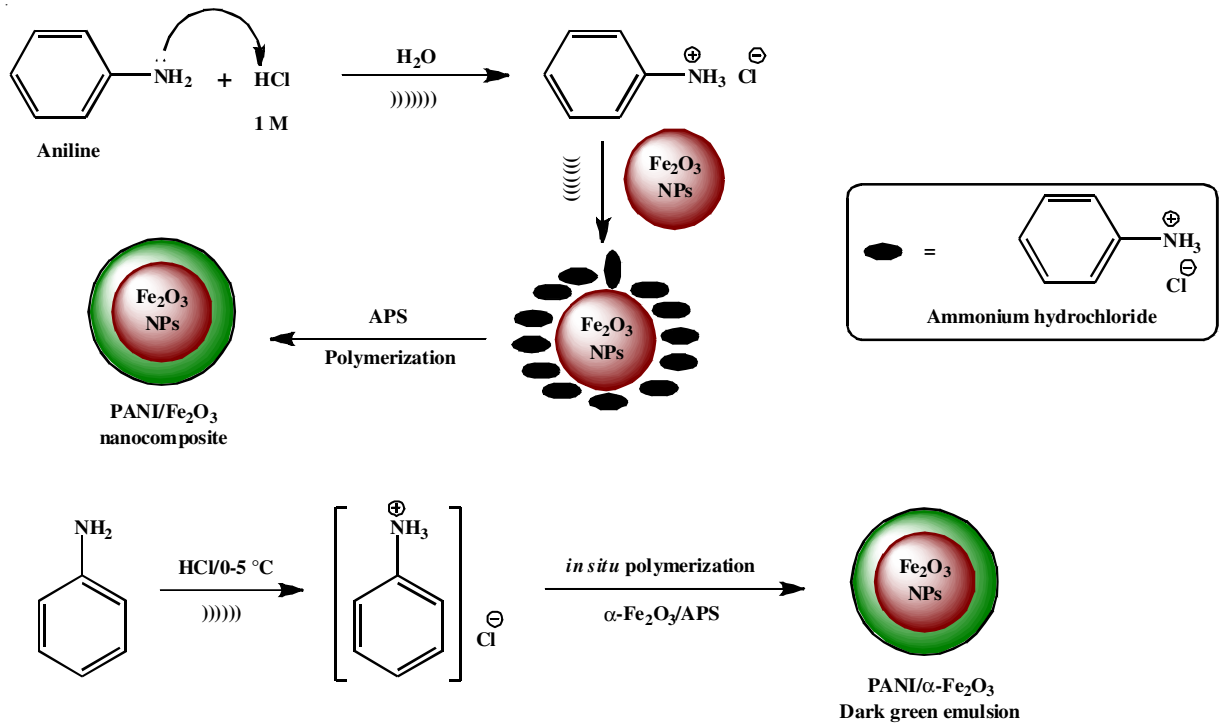

Scheme-II: Ultrasonic synthesis of PANI/HAM$_3$ nanocomposite

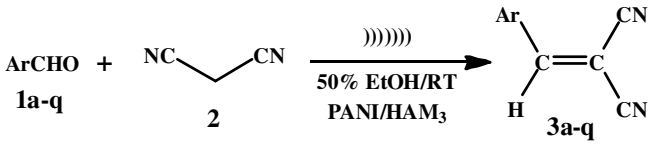

Scheme-III: Knovenagel synthesis

Spectral analysis of selected molecules

2-(3-Nitrobenzylidene malononitrile) (3a): FTIR (KBr, ν_{max}, cm^{-1}): 3107, 2225, 1610, 1595, 1529, 1479; ^{1}H NMR (500 MHz, DMSO-d_6): δ 8.76 (s, 1H), 8.48 (d, 1H), 8.33 (d, 1H), 7. 92 (t, 1H), 7.89 (s, 1H); ^{13}C NMR (500 MHz, DMSO-d_6): δ 159.71, 148.47, 136.30, 132.89, 131.62, 128.38, 125.32, 114.10, 113.05 and 85.35.

2-(4-Chlorobenzylidene malononitrile) (3b): FTIR (KBr, ν_{max}, cm^{-1}): 3183, 2135, 1604, 1584, 1560, 1014; ^{1}H NMR (500 MHz, DMSO-d_6): δ 8.56 (s, 1H), 7.95 (d, 2H, J = 8.0 Hz), 7.74 (d, 2H, J = 8.0 Hz); ^{13}C NMR (500 MHz, DMSO-d_6): δ 159.22, 139.50, 131.86, 130.51, 129.31, 114.11, 113.70, 84.66.

2-(4-Hydroxy-3-methoxybenzylidene malononitrile) (3c): FTIR (KBr, ν_{max}, cm^{-1}): 3188, 2125, 1606, 1582, 1550, 1012; ^{1}H NMR (500 MHz, DMSO-d_6): δ 8.26 (s, 1H), 7.65 (d, 1H), 7.51 (dd 1H), 6.98 (d 1H), 3.80 (s 3H); ^{13}C NMR (500 MHz, DMSO-d_6): δ 161.02, 154.50, 148.38, 128.20, 123.46, 116.64, 115.61, 114.84, 113.54, 75.28, 55.92.

2-(4-Ethoxybenzylidene malononitrile) (3d): FTIR (KBr, ν_{max}, cm^{-1}): 3188, 2225, 1606, 1582, 1550, 1014; ^{1}H NMR (500 MHz, DMSO-d_6): δ 8.38 (s, 1H), 7.98 (d, 2H), 7.18 (d, 2H), 4.18 (q, 3H), 1.37 (t, 3H); ^{13}C NMR (500 MHz, DMSO-d_6): δ 161.22, 158.3, 131.21, 129.50, 124.86, 114.11, 113.70, 84.66, 68.11, 43.12.

2-(4-Hydroxybenzylidene malononitrile) (3e): FTIR (KBr, ν_{max}, cm^{-1}): 3356, 3331, 3094, 3078, 3031, 2933, 2226, 1565, 1495; ^{1}H NMR (500 MHz, DMSO-d_6): δ 11.02 (1H, br.), 8.31 (s, 1H), 7.90 (d, 2H), 6.97 (d, 2H); ^{13}C NMR (500 MHz, DMSO-d_6): δ 164.42, 160.98, 148.38, 134.35, 123.36, 117.61, 115.58, 114.67, 75.52, 40.48.

2-(4-Fluro benzylidene malononitrile) (3f): FTIR (KBr, ν_{max}, cm^{-1}): 3500, 3331, 3094, 2224, 1615, 1489, 1226, 686; ^{1}H NMR (500 MHz, DMSO-d_6): δ 8.55 (1H, s) 8.05 (d, 2H), 7.50 (d, 2H).

2-(4-Ethyl benzylidene malononitrile) (3h): FTIR (KBr, ν_{max}, cm^{-1}): 3340, 3094, 2224, 1620, 1489, 1233; ^{1}H NMR (500 MHz, DMSO-d_6): δ 8.49 (1H, s) 7.89 (d, 2H), 7.47 (d, 2H), 2.71 (q, 2H), 1.20(t, 3H).

2-(3,4,5-Trimethoxy benzylidene malononitrile) (3i): FTIR (KBr, ν_{max}, cm^{-1}): 2943, 2225, 1568, 1500, 1249, 1128; ^{1}H NMR (500 MHz, DMSO-d_6): δ 8.41 (1H, s) 7.38 (s, 2H), 3.81 (s, 9H).

2-(2-Cyano benzylidene malononitrile) (3j): FTIR (KBr, ν_{max}, cm^{-1}): 3043, 2224, 1560, 1500, 1249; ^{1}H NMR (500 MHz, DMSO-d_6): δ 8.90 (s, 1H), 8.33 (1H, d) 7.88 (s, 1H), 7.80 (dd, 1H), 7.79 (d, 1H).

2-(Benzylidene malononitrile) (3k): FTIR (KBr, ν_{max}, cm^{-1}): 3182, 2224, 1691, 1592, 1090; ^{1}H NMR (500 MHz, DMSO-d_6): δ 78.56 (s, 1H), 7.96 (d, 2H), 7.69 (t, 1H), 7.63 (t, 2H) J = 7.60 Hz), 7.64 (t, 1H, J = 7.60 Hz), 7.27 (t, 2H, J = 7.60 Hz), 7.12 (s, 1H); ^{13}C NMR: δ 159.98, 134.35, 130.89, 129.45, 113.56, 112.55, 82.78.

RESULTS AND DISCUSSION

Efficiency of ultrasonic synthesis: A control reaction was performed under various reaction conditions by conventional and ultrasonic green route. Table-1 compares the efficiency of an ultrasonic synthesis concerning time, yield and temperature

TABLE-1
EFFICIENCY OF ULTRASONIC SYNTHESIS THAN OTHER METHODS

Entry	Reaction conditions	Time (min)	Yield (%)
1	Reflux at 60-70 °C	100	60
2	Magnetic stirring at room temp.	80	72
3	Magnetic stirring at 60-70 °C	85	68
4	Ultrasonic at room temp.	12	98
5	Ultrasonic at 60 °C	20	97

[a]Reaction conditions: Aromatic aldehyde (1 mmol), malononitrile (1 mmol), PANI/HAM_3 (20 mg) and 5 mL aqueous ethanol (50% v/v)

with the competence of other methods of synthesis for control reaction. The results obtained showed that time taken for the ultrasonic reaction was much shorter and the yield of the product obtained was greater under ultrasound irradiation reaction conditions than the conventional methods.

Screening of catalyst and its amount: A control reaction experiment was performed without catalyst resulting in low yields of products and high reaction time (Fig. 1). Various nanomaterials such as α-Fe_2O_3 prepared without any capping agent (HAM_1), hematite prepared by sol gel method (HAM_2), HAM_3, PANI, PANI/HAM_3, magnetite (Fe_3O_4), maghematite (γ-Fe_2O_3) nanoparticles and reaction without catalyst were investigated and compared for yields of the product and time required for the reaction completion under ultrasound irradiation. The control reaction in the presence of PANI/HAM_3 afforded the product quickly with higher yield in aqueous ethanol under ultrasound conditions.

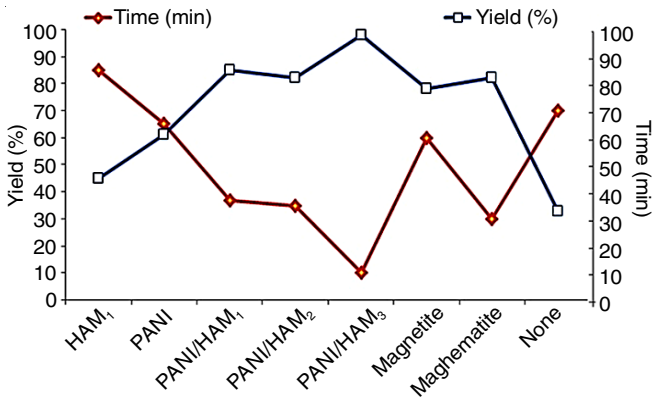

Fig. 1. Screening of catalyst

The effect of PANI/HAM_3 catalyst loading on the yield of product was investigated by varying the amount of catalyst from 5 to 30 mg (Fig. 2). The result showed that the yield of the product increased with an increase in the amount of catalyst up to 20 mg and then thereafter no change in practical yield was observed with an increase in the amount of catalyst up to 30 mg.

Effect of solvent and temperature: The control reaction was carried out in solvent-free conditions as well as in the presence of various solvents. The solvent-free conditions *i.e.* solid-state reaction provided a very poor yield of the product. Fig. 3 compares the results obtained for yield and time taken for the reaction and confirms that (50% v/v) aqueous ethanol is the best choice of solvent for control reaction. The effect of

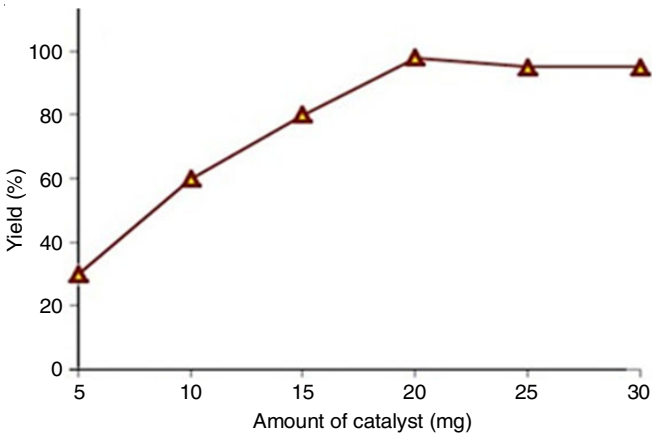

Fig. 2. Amount of PANI/HAM_3 catalyst

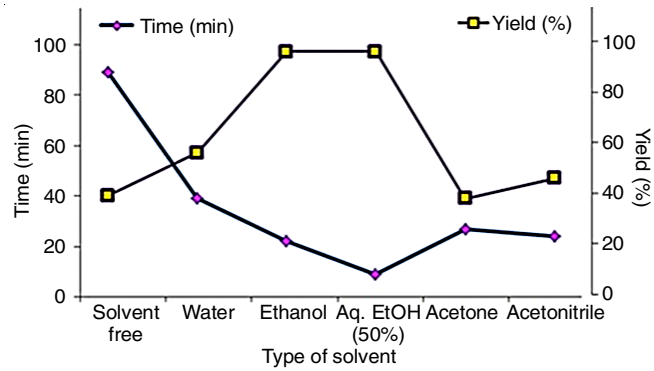

Fig. 3. Solvent effect

temperature (Table-2) was studied by carrying out the control reaction at different temperatures in the presence of PANI/HAM_3 nanocatalyst in aqueous ethanol. It was observed that the maximum yield in a short time was obtained at about 25-30 ºC.

TABLE-2
EFFECT OF TEMPERATURE

Temp. (°C)	Time (min)	Yield (%)
Room temp. (25-30)	12	98
30-40	12	98
40-50	18	97
50-60	20	97

Recycling efficiency of PANI/HAM_3 as catalyst: The catalytic efficiency of PANI/HAM_3 was investigated in repetitive reaction cycles. To investigate efficiency, after each cycle, the catalyst was separated, sonicated and washed with ethanol and deionized water, then subsequently used for the next reaction after drying. It is observed that the catalytic activity remains unchanged for the first five cycles and then a slight decrease in the yield was observed up to six cycles (Fig. 4). This suggests that PANI/HAM_3 remains active at least up to five cycles without much loss in its catalytic activity.

FTIR studies: The chemical composition of the prepared nanomaterials *i.e.* α-Fe_2O_3 (HAM_3) and PANI/HAM_3 was confirmed by FTIR spectroscopic analysis. FTIR spectra of α-Fe_2O_3 shows (Fig. 5a) characteristic peaks at 486 cm^{-1} and 585 cm^{-1} were attributed to stretching vibration frequency of Fe-O bond

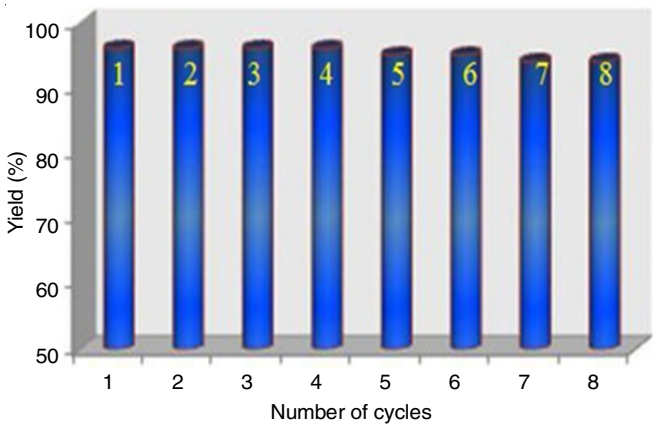

Fig. 4. Recycling efficiency of PANI/HAM_3 catalyst

in HAM_3 nanoparticles. The broad peak at 3385 cm^{-1} observed due to the O-H stretching vibrations [28,29]. FTIR spectrum of PANI/HAM_3 nanocomposite (Fig. 5b) shows the characteristic bands at 1590 cm^{-1} and 1510 cm^{-1} attributed to quinoid and benzenoid ring stretching vibrations, respectively confirming the structure of PANI [30-32]. The absorption band at 1250 cm^{-1} and 1320 cm^{-1} correspond to the C-N stretching of PANI. The absorption bands at 760 cm^{-1} and 510 cm^{-1} were attributed to the bending vibrations of C-N for 1,4-disubstituted benzene ring and bending vibrations of benzene ring, respectively. The peak at 590 cm^{-1} indicated the presence of Fe-O stretching frequency in PANI/HAM_3 nanocomposite [33,34].

XRD studies: In order to confirm the composition and phase of iron oxide prepared, X-ray diffraction (XRD) study was carried out. The XRD pattern of α-Fe_2O_3 (Fig. 6a) show the sharp diffraction peaks indicating good crystallinity and rhombohedral structure of most stable form of iron oxide *i.e.* hematite nanoparticles. All the diffraction peaks of hematite nanoparticles are in excellent agreement with JCPDS no. 33-0664 [35]. No characteristic peaks for impurities were detected indicating pure form of α-Fe_2O_3. XRD diffraction patterns of PANI/HAM_3 nanocomposite (Fig. 6b) show broad reflection at 25.33°, which is a characteristic peak of PANI. Apart from a broad peak of PANI, major diffraction peaks for the hematite corresponding to (104), (113), (110), (024) and (116) planes at appropriate 2θ were observed, which confirms the formation of PANI/HAM_3 nanocomposite. The particle size was found to be 30-50 nm determined by Schererr's formula:

$$\text{Scherer formula (D)} = \frac{0.891\lambda}{\beta\cos\theta}$$

where, D is the average particle size, λ is the wavelength (1.54 Å) of X-rays, θ is the diffraction angle and β is the full-width at half maximum of an observed peak. The broadening of the peaks in PANI/HAM_3 point out that the composite particles obtained were of nanometer scale. It is also observed that there is a slight shift of peaks for characteristic peaks for polyaniline in PANI/HAM_3 composite to higher 2θ indicating an interaction of PANI with hematite in the nanocomposite.

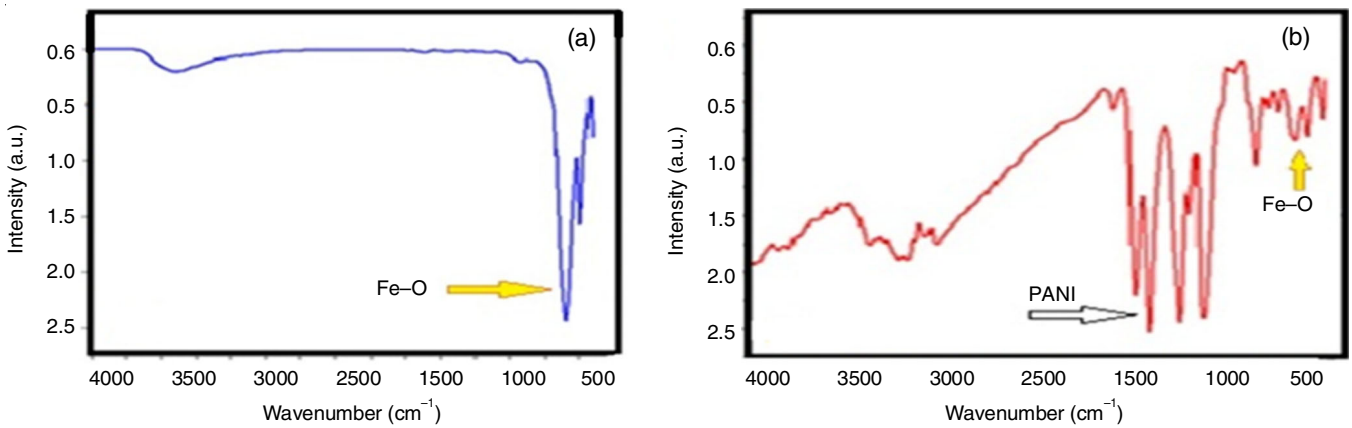

Fig. 5. FTIR (a) HAM_3 (b) PANI/HAM_3

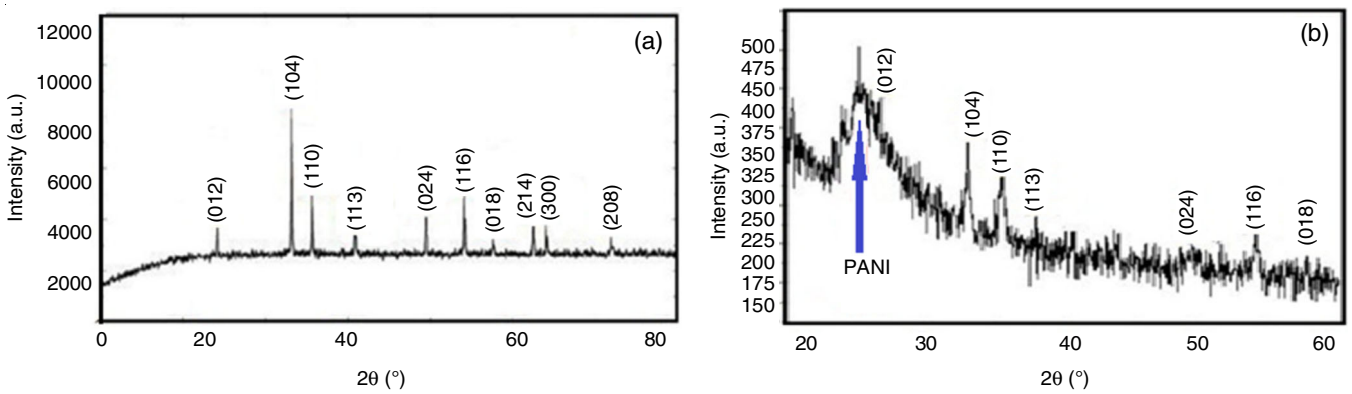

Fig. 6. XRD (a) HAM_3 (b) PANI/HAM_3

Morphological and particle size studies

FESEM studies: The SEM image and particle size distribution of synthesized α-Fe_2O_3 and PANI/HAM_3 are shown in Fig. 7. The images obtained for hematite shows the spherically rippled cauliflower like microstructures containing slightly agglomerated α-Fe_2O_3 nanospheres with a uniform diameter of 30-50 nm (Fig. 7a). The SEM micrograph of PANI/HAM_3 nanocomposite (Fig. 7b) indicates the formation of fibrous material of PANI, with uniformly dispersed nanospheres of hematite. The ultrasonication during synthesis of hybrid composite material helped in the better particle separation and uniform distribution of hematite nanoparticles in the fibrous matrix of PANI [31-33].

Dynamic light scattering (DLS) technique: Fig. 8 demonstrates the plot of DLS for HAM_3 and PANI/HAM_3 nanocomposite. The hydrodynamic diameter of the hematite nanoparticles is 922.5 nm and that of composite particles is 66.39 nm. Due to the hydrophilic nature of hematite and aggregate formation, its particle diameter is much greater than that of PANI/HAM_3 nanocomposite. The polydispersity index of hematite is very low indicating the narrow size distribution of hematite nanoparticles [36-38].

Ultrasonic synthesis of Knoevenagel condensation: The PANI/HAM_3 was used as a heterogeneous catalyst for C-C bond formation, Knoevenagel condensation reaction over various substituted aromatic aldehydes (**Scheme-III**). The yields, time

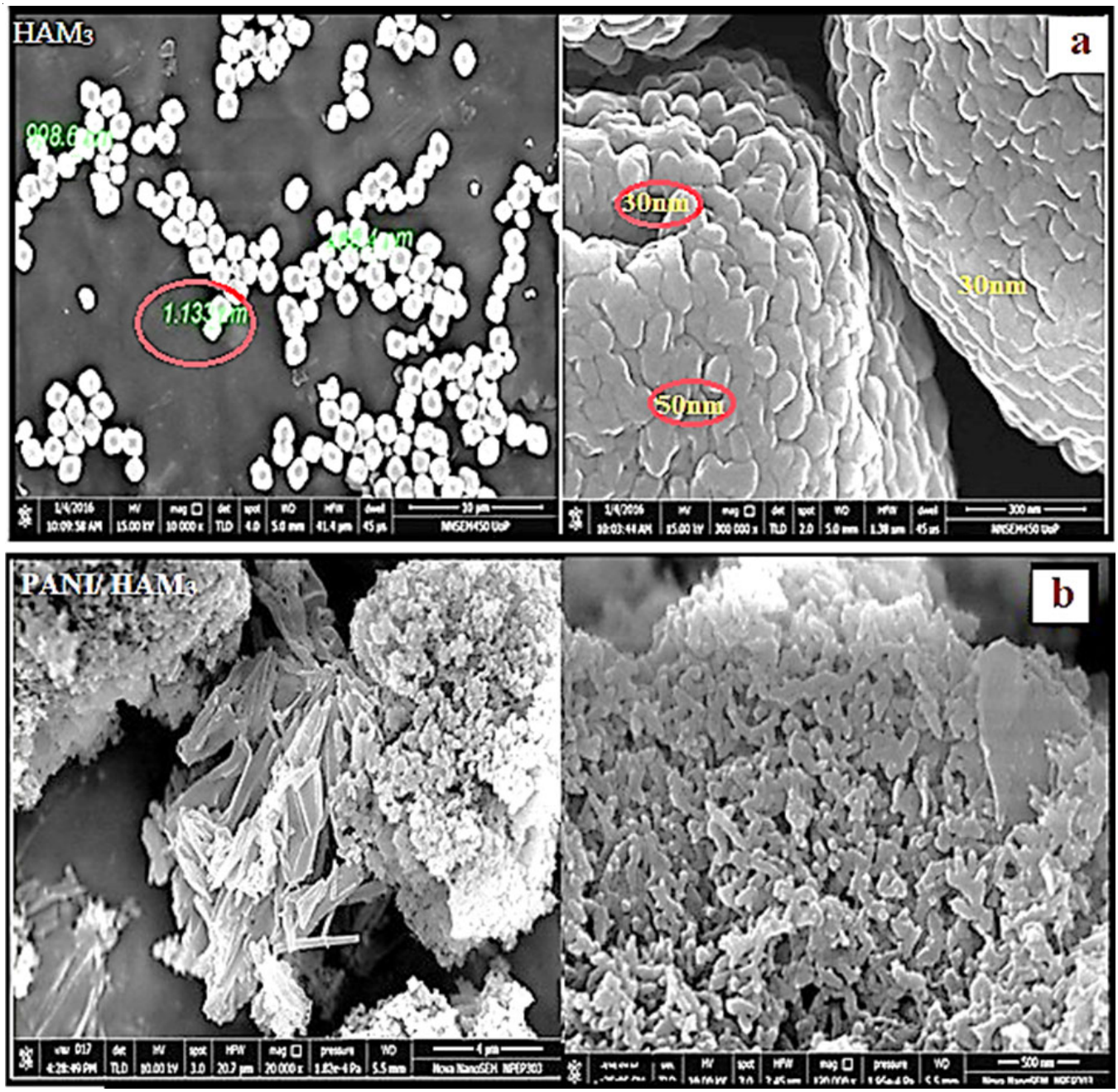

Fig. 7. FESEM (a) HAM_3 (b) PANI/HAM_3

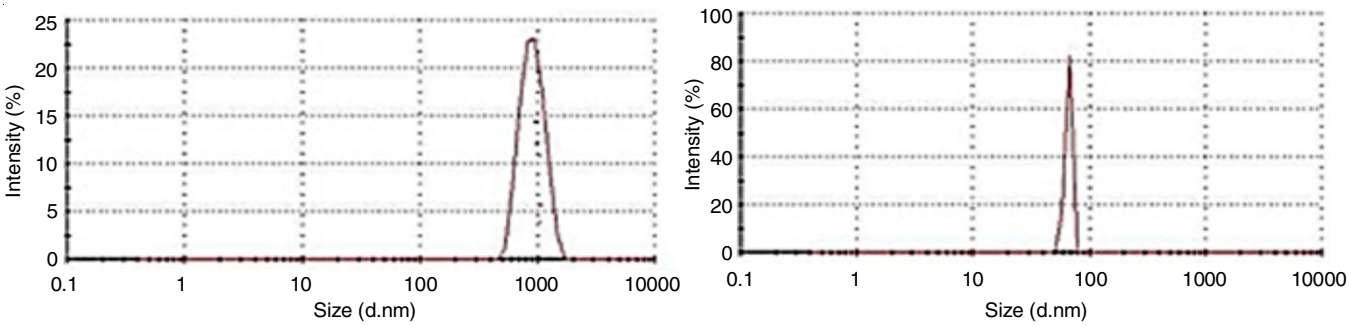

Fig. 8. DLS images of (a) HAM_3 (b) $PANI/HAM_3$

and physical constants of various products obtained were characterized. It was observed that the reaction proceeds almost exclusively at room temperature (25-30 ºC) under ultrasonication. For all the substrates, very high yields of the condensation products were obtained within 8-20 min. It was observed that aromatic aldehydes containing electron-withdrawing groups react at a faster rate than aromatic aldehydes containing electron donating groups under base-free *i.e.* neutral conditions.

Comparison of $PANI/HAM_3$ nanocatalyst with recently published works for the Knoevenagel condensation of benzaldehyde and malononitrile: In present study, our aim was to develop an ultrasonic mediated quick condensation in neutral reaction medium in ecofriendly solvent at room temperature by using reusable efficient economical catalyst system than existing choices [39,40]. Viswanadham *et al.* [41] introduced a vanadium containing PMA ($PMoV_3$) catalyst system for the Knoevenagel reaction under a solvent free conditions, which required longer time to achieve 86% yield of product. Lee *et al.* [42] reported a sluggish Knoevenagel condensation by using $MOF\text{-}NH_2$ as catalyst in the presence of DMF as solvent at 80 ºC in 270 min with 51% yield. A new expensive MOF-Pd catalyst was developed by Ezugwu *et al.* [43] for quick condensation reaction. Shirini *et al.* [44] reported application of 2-aminoethanesulfonic acid as catalyst for condensation in water under reflux conditions with poor yields. Maleki *et al.* [45] reported a magnetically separable Fe_3O_4-cysteamine hydrochloride catalysis, with longer reaction times. Sakthivel *et al.* [46] reported the reaction catalyzed by using chitosan in ethanol at 40 ºC for 360 min attaining 99% conversion. Sen & Dhakshinamoorthy [47] utilized a complex and expensive Rh-Pt/TC@GO system at room temperature for the fast condensation reaction with excellent yield. Lolak *et al.* [48] exploited highly luxurious palladium-nickel alloy catalyst at room temperature for quick condensation reaction, whereas Patel *et al.* [49] recycled FeNPs /PPD@rGO for the Knoevenagel reaction in toluene at 40 ºC in 180 min to get 100% yield of the condensation product. As demonstrated in Table-3, it was perceived that the ultrasonically prepared, $PANI/HAM_3$ nanocatalyst was used first time and has offered one of the best catalytic performances for the quick Knoevenagel condensation with high yields as compared with that of other catalyst systems reported in the literature.

Plausible mechanism: Ultrasound spreads *via* a chain of expansion and compression cycles induced in a liquid medium. Accordingly cavities grow and collapse in different stages.

TABLE-3
ASSESSMENT OF THE $PANI/HAM_3$ NANOCATALYST WITH RECENTLY PUBLISHED WORKS FOR THE KNOEVENAGEL REACTION OF BENZALDEHYDE AND MALONONITRILE

Catalyst	Time (min)	Reaction conditions	Yield (%)	Ref.
$PMoV_3$	46	Solvent free/70 °C	86	[41]
$MOF\text{-}NH_2$	270	DMF/80 °C	51	[42]
MOF-Pd	05	DMSO/RT	43	[43]
Taurine	14	Water/100 °C	86	[44]
Fe_3O_4-cysteamine hydrochloride	20	aq. EtOH/50 °C	93	[45]
Chitosan	360	EtOH/40 °C	>99	[46]
RhPt/TC @GO	10	aq. MeOH/RT	>99	[47]
GO @ PdNi	08	aq. EtOH/RT	95	[48]
FeNPs/PPD@rGO	180	Toluene/40 °C	100	[49]
$PANI/HAM_3$	15	aq. EtOH/RT	98	Present work

Eventually, cavities collapse energetically, producing high pressures with local heating for very short lifetimes [50]. The formation of cavities or bubbles generating shock waves, are responsible for most of the ultrasonic physical and chemical effects [51]. These effects cause the dispersion of nanoparticles and can avoid their agglomeration. Also, the separation of the materials (reactants) attached to the active surface leads to an increase in the rate and efficiency of the reaction. Hence, ultrasound assisted methods are a green methodology under mild reaction conditions, leading to high reaction yields and lower levels of pollution. In heterogeneous systems, the reactions are influenced primarily through the mechanical effects of cavitation, such as surface cleaning, particle size reduction and improved mass transfer. When cavitation occurs in a liquid near a solid catalyst surface, the dynamics of cavity collapse change intensely [52,53]. The efficiency of the ultrasonic method is explained in Table-1, which makes it the best suitable process for Knoevenagel condensation than other reported methods. A plausible mechanism explaining the aforementioned results as illustrated in **Scheme-IV**. The process represents a typical cascade of Knoevenagel condensation reaction in the presence of a new recyclable $PANI/HAM_3$ nanocatalyst, acting as a Lewis acid efficiently under ultrasound waves. The catalyst acts as an electron acceptor and ultrasound waves facilitate the condensation reaction between aldehyde and malononitrile. The dipolar form of PANI also increases the acidic characters of the catalyst which stabilizes the tautomeric form of malononitrile as shown in **Scheme-IV**. A lone pair on

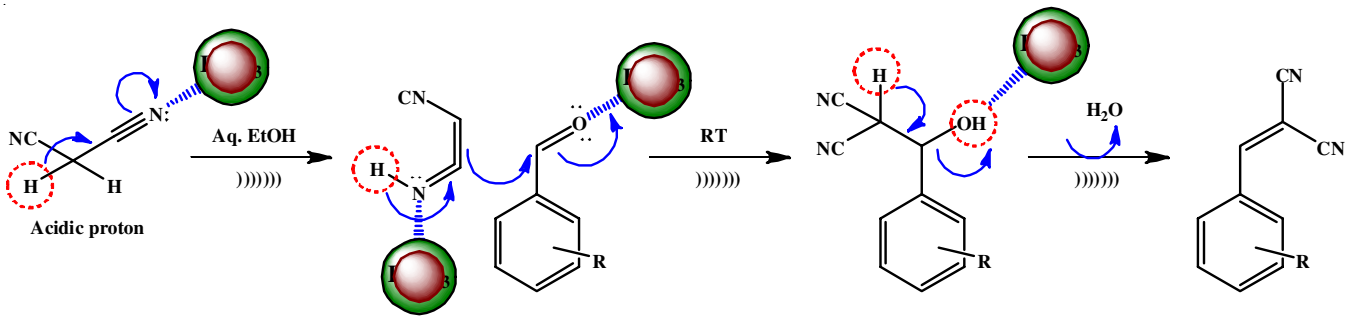

Scheme-IV: Plausible mechanism

the oxygen of carbonyl group forms a coordinate bond with electron-deficient sites of catalyst and increases the nucleophilic character as well as the reactivity of the carbonyl group. The ultrasound cavitation keeps the catalyst particles well dispersed throughout the reaction mixture and also minimizes the agglomeration of the nanoparticles, which increases the surface area of the catalyst and hence increases the rate of condensation as well as improves the yield of the reaction. The ultrasound irradiation accelerates the spherical nanoparticles significantly by the shockwave that occurs during the explosive growth of a cavity on the particle surface. Ultrasound also activates the reaction mixture by inducing high local temperature and pressure generated inside the cavitation bubble when it collapses and enhances the rate of the reaction. The active sites of catalyst can be attributed to Lewis-base-type species located in the PANI/HAM_3 matrixes. Initially, an acidic proton is abstracted from the active methylene group by a Lewis-base site, yielding a stable anion. Spontaneously, the original base site is converted into a protonated position (conjugate acid). Consequently, this anion makes a nucleophilic attack on the carbonyl carbon atom of the aldehyde, generating an oxyanion. Subsequently, abstracting H^+ from the protonated position of catalyst and removing an H_2O molecule, the oxyanion goes into the corresponding condensation product under ultrasonic conditions at ambient temperature in aqueous ethanol [54].

Conclusion

In this work, an ultrasound-assisted modest green synthetic method was introduced, using a new PANI/HAM_3 nanocatalyst and applied to the Knoevenagel condensation reaction of a wide range of aromatic aldehydes with malononitrile. The PANI/HAM_3 heterogeneous catalyst system showed an excellent catalytic performance and can be recovered easily *via* centrifuging. It can also be reused six times for the aforementioned transformation with no considerable loss of activity. To analyze the catalytic activity of the prepared catalyst, many parameters of the condensation reaction were examined, such as the types of catalyst, the dosage of catalyst and solvent. On the basis of the results observed, ultrasonic conditions at 25-30 ºC, the use of ethanol/water (1:1) as solvent and PANI/HAM_3 nanocatalyst were selected for carrying out the C-C bond formation reaction *via* condensation reaction. Ultrasound, due to cavitation effects, can generate effective intensity in the reaction process; causing physical and chemical effects. These effects cause the dispersion of PANI/HAM_3 nanoparticles, which can avert them from agglomeration. Also, the separation of the reacting materials attached to the active surface leads to an increase in the rate and efficiency of the reaction as compared to other conventional methods of synthesis.

ACKNOWLEDGEMENTS

The authors are thankful to the UGC, India for financial support under the minor research project. Thanks to the IIT Bombay and Central Instrumentation Facility, Savitribai Phule Pune University, Pune, India for their technical support.

CONFLICT OF INTEREST

The authors declare that there is no conflict of interests regarding the publication of this article.

REFERENCES

1. S.V. Sancheti and P.R. Gogate, *Ultrason. Sonochem.*, **36**, 527 (2017); https://doi.org/10.1016/j.ultsonch.2016.08.009
2. E. Mosaddegh, *Ultrason. Sonochem.*, **20**, 1436 (2013); https://doi.org/10.1016/j.ultsonch.2013.04.008
3. B. Banerjee, *Ultrason. Sonochem.*, **35**, 1 (2017); https://doi.org/10.1016/j.ultsonch.2016.09.023
4. J.S. Ghomi and Z. Akbarzadeh, *Ultrason. Sonochem.*, **40**, 78 (2018); https://doi.org/10.1016/j.ultsonch.2017.06.022
5. P. Qiu, B. Park, J. Choi, B. Thokchom, A.B. Pandit and J. Khim, *Ultrason. Sonochem.*, **45**, 29 (2018); https://doi.org/10.1016/j.ultsonch.2018.03.003
6. S.Y. Hao, Y.H. Li, J. Zhu and G.H. Cui, *Ultrason. Sonochem.*, **40**, 68 (2018); https://doi.org/10.1016/j.ultsonch.2017.06.028
7. R. Taheri-Ledari, J. Rahimi and A. Maleki, *Ultrason. Sonochem.*, **59**, 104737 (2019); https://doi.org/10.1016/j.ultsonch.2019.104737
8. S. Majhi, *Ultrason. Sonochem.*, **77**, 105665 (2021); https://doi.org/10.1016/j.ultsonch.2021.105665
9. A.R. Khosropour, *Ultrason. Sonochem.*, **15**, 659 (2008); https://doi.org/10.1016/j.ultsonch.2007.12.005
10. V.V. Chabukswar, M.A. Bora, P.B. Adhav, B.B. Diwate and S. Salunke-Gawali, *Polym. Bull.*, **76**, 6153 (2019); https://doi.org/10.1007/s00289-019-02703-4
11. J.T. Li, H.J. Zang, L.H. Meng, L.J. Li, Y.H. Yin and T.S. Li, *Ultrason. Sonochem.*, **8**, 93 (2001); https://doi.org/10.1016/S1350-4177(00)00067-5
12. M.A. Bora, P.B. Adhav, B.B. Diwate, D.S. Pawar, S. Dallavalle and V.V. Chabukswar, *Polym. Plastics Technol. Mater.*, **58**, 1545 (2019); https://doi.org/10.1080/25740881.2018.1563131
13. C. Goswami, K.K. Hazarika and P. Bharali, *Mater. Sci. Ener. Technol.*, **1**, 117 (2018); https://doi.org/10.1016/j.mset.2018.06.005
14. J.T. Li, S.X. Wang, G.F. Chen and T.S. Li, *Curr. Org. Synth.*, **2**, 415 (2005); https://doi.org/10.2174/1570179054368509

15. P.N. Uyen, K.A.T. Li and N.T. Phan, *ACS Catal.*, **12**, 120 (2011); https://doi.org/10.1021/cs1000625
16. T.S. Saleh, M.A. Eldebss and H.M. Albishri, *Ultrason. Sonochem.*, **19**, 49 (2012); https://doi.org/10.1016/j.ultsonch.2011.05.003
17. K.P. Guzen, A.S. Guarezemini, A.T.G. Órfão, R. Cella, C.M.P. Pereira and H.A. Stefani, *Tetrahedron Lett.*, **48**, 1845 (2007); https://doi.org/10.1016/j.tetlet.2007.01.014
18. S. Kotha and P. Khedkar, *Chem. Rev.*, **112**, 1650 (2012); https://doi.org/10.1021/cr100175t
19. Z. Zhang, Z. Zha, C. Gan, C. Pan, Y. Zhou, Z. Wang and M.-M. Zhou, *J. Org. Chem.*, **71**, 4339 (2006); https://doi.org/10.1021/jo060372b
20. Q. Liu, H. Ai and Z. Li, *Ultrason. Sonochem.*, **18**, 477 (2011); https://doi.org/10.1016/j.ultsonch.2010.09.003
21. J. McNulty, J. Steere and S. Wolf, *Tetrahedron Lett.*, **39**, 8013 (1998); https://doi.org/10.1016/S0040-4039(98)01789-4
22. K.C. Majumdar, A. Taher and S. Ponra, *Tetrahedron Lett.*, **51**, 147 (2010); https://doi.org/10.1016/j.tetlet.2009.10.108
23. A. Ibrahim and B.A. Abubakar, *African J. Pure Appl. Chem.*, **7**, 114 (2013); https://doi.org/10.5897/AJPAC12.002
24. T. Jin, J. Xiao, S. Wang and T. Li, *Ultrason. Sonochem.*, **11**, 393 (2004); https://doi.org/10.1016/j.ultsonch.2003.10.002
25. J. Safari and L. Javadian, *Ultrason. Sonochem.*, **22**, 341 (2015); https://doi.org/10.1016/j.ultsonch.2014.02.002
26. M.B. Gawande, A. Goswami, F.X. Felpin, X.T. Asefa, X. Huang, R. Silva, X. Zou, R. Zboril and R.S. Varma, *Chem. Rev.*, **116**, 3722 (2016); https://doi.org/10.1021/acs.chemrev.5b00482
27. A.A. Spasov, I.N. Yozhitsa, L.I. Bugaeva and V.A. Anisimova, *Pharm. Chem. J.*, **33**, 232 (1999); https://doi.org/10.1007/BF02510042
28. Y. Jiang, X.-M. Meng, W.-C. Yiu, J. Liu, J.-X. Ding, C.-S. Lee and S.-T. Lee, *J. Phys. Chem. B*, **108**, 2784 (2004); https://doi.org/10.1021/jp035595+
29. R.G.J. Strens and B.J. Wood, *Mineral. Mag.*, **328**, 509 (1987).
30. K.M. Molapo, P.M. Ndangili, R.F. Ajayi, G. Mbambisa, S.M. Mailu, N. Njomo, M. Masikini, P. Baker and E.I. Iwuoha, *Int. J. Electrochem. Sci.,* **7**, 11859 (2012).
31. Z. Ai, K. Deng, Q. Wan, L. Zhang and S. Lee, *J. Phys. Chem. C*, **114**, 6237 (2010); https://doi.org/10.1021/jp910514f
32. F.N. Sayed and V. Polshettiwar, *Sci. Rep.*, **5**, 09733 (2015); https://doi.org/10.1038/srep09733
33. A.P. Roberts, Q. Liu, C.J. Rowan, L. Chang, C. Carvallo, J. Torrent and C.-S. Horng, *J. Geophys. Res.*, **111**, B12S3 (2006); https://doi.org/10.1029/2006JB004715
34. H.J. Song, X. Zhang, T. Chen and X. Jia, *Ceram. Int.*, **40**, 15595 (2014); https://doi.org/10.1016/j.ceramint.2014.07.037
35. G. Marciniak, A. Delgado, G. Leclerc, J. Velly, N. Decker and J. Schwartz, *J. Med. Chem.*, **32**, 1402 (1989); https://doi.org/10.1021/jm00126a042
36. D. Enders, E. Muller and A.S. Demir, *Tetrahedron Lett.*, **29**, 6437 (1988); https://doi.org/10.1016/S0040-4039(00)82366-7
37. E. Knoevenagel, *Ber. Dtsch. Chem. Ges.*, **27**, 2345 (1894); https://doi.org/10.1002/cber.189402702229
38. G. Jones, *Org. React.*, **15**, 204 (2011); https://doi.org/10.1002/0471264180.or015.02
39. J. Xu, K. Shen, B. Xue and Y.-X. Li, *J. Mol. Catal. Chem.*, **372**, 105 (2013); https://doi.org/10.1016/j.molcata.2013.02.019
40. V.K. Harika, H.K. Sadhanala, I. Perelshtein and A. Gedanken, *Ultrason. Sonochem.*, **60**, 104804 (2020); https://doi.org/10.1016/j.ultsonch.2019.104804
41. B. Viswanadham, P. Jhansi, K.V.R. Chary, H. Friedrich and S. Singh, *Catal. Lett.*, **146**, 364 (2016); https://doi.org/10.1007/s10562-015-1646-9
42. I.M. Lee, A. Taher, D.J. Lee and B.K. Lee, *Synlett*, **27**, 1433 (2016); https://doi.org/10.1055/s-0035-1561356
43. C.I. Ezugwu, B. Mousavi, M.A. Asraf, Z. Luo and F. Verpoort, *J. Catal.*, **344**, 445 (2016); https://doi.org/10.1016/j.jcat.2016.10.015
44. F. Shirini and N. Daneshvar, *RSC Adv.*, **6**, 110190 (2016); https://doi.org/10.1039/C6RA15432H
45. R. Maleki, E. Kolvari, M. Salehi and N. Koukabi, *Appl. Organomet. Chem.*, **31**, e3795 (2017); https://doi.org/10.1002/aoc.3795
46. B. Sakthivel and A. Dhakshinamoorthy, *J. Colloid Interface Sci.*, **485**, 75 (2017); https://doi.org/10.1016/j.jcis.2016.09.020
47. B. Sen, E.H. Akdere, A. Savk, E. Gültekin, Ö. Parali, H. Göksu and F. Sen, *Appl. Catal. B*, **225**, 148 (2018); https://doi.org/10.1016/j.apcatb.2017.11.067
48. N. Lolak, E. Kuyuldar, H. Burhan, H. Goksu, S. Akocak and F. Sen, *ACS Omega*, **4**, 6848 (2019); https://doi.org/10.1021/acsomega.9b00485
49. D. Patel, R. Vithalani and C.K. Modi, *New J. Chem.*, **44**, 2868 (2020); https://doi.org/10.1039/C9NJ05821D
50. R.B. Nasir Baig and S. Rajender Varma, *Chem. Soc. Rev.*, **41**, 1559 (2012); https://https://doi.org/10.1039/c1cs15204a
51. H. Veisi, A. Mirzaei and P. Mohammadi, *RSC Adv.*, **9**, 41581 (2019); https://doi.org/10.1039/C9RA08809A
52. F. Chang, J. Wang, J. Luo, J. Sun and X. Hu, *J. Colloid Interface Sci.*, **468**, 284 (2016); https://doi.org/10.1016/j.jcis.2016.01.077
53. G. Brahmachari, I. Karmakar and K. Nurjamal, *ACS Sustain. Chem. Eng.*, **6**, 11018 (2018); https://doi.org/10.1021/acssuschemeng.8b02448
54. S. Saranya, S. Radhika, C.M. Afsina Abdulla and G. Anilkumar, *J. Heterocycl. Chem.*, **58**, 1570 (2021); https://doi.org/10.1002/jhet.4261